Bound State Solutions of the Klein-Gordon Equation for Strong Potentials

Wolfgang Fleischer and Gerhard Soff
Gesellschaft für Schwerionenforschung mbH, Darmstadt

Z. Naturforsch. **39a**, 703–719 (1984); received January 28, 1984

We explicitly construct normalized solutions of the Klein-Gordon equation for various types of attractive potentials. Our computed binding energies of several short- and long-range potentials are compared with results published by different authors. Special emphasis is laid on the determination of critical potential strengths, i.e. the onset of spontaneous pair creation of spin-0 particles. In the vicinity of these critical values the single-particle interpretation breaks down. The phenomenon of simultaneous particle and antiparticle binding in a short-range potential is investigated.

1. Introduction

Our research concerning the behaviour of a strongly bound spin-0 particle was basically motivated by the work of Pieper and Greiner [1] who solved the Dirac equation for a strong Coulomb potential. In their publication [1] it was demonstrated that spontaneous electron-positron pair creation takes place if the charge number Z of a realistic finite size nucleus exceeds a specific critical value which amounts to $Z_{cr} \simeq 170$ for an electron in the 1s-state. It was pointed out that this fascinating process is equivalent to a transition from a neutral vacuum to a charged vacuum. An experimental proof of these underlying theoretical ideas is presently performed by measurements of the positron emission in collisions of very heavy ions such as $_{92}U + _{92}U$. A concise but complete summary of the atomic physics and quantumelectrodynamical problems in superheavy colliding systems is given in [2]. The current theoretical status and its experimental verification concerning the determination of critical nuclear charges and the spontaneous positron emission has been reviewed recently in [3].

It is almost compelling to extend these examinations to a Klein-Gordon particle (pion, etc.) confined in an attractive potential with a binding energy comparable to its rest mass. The history of the corresponding theoretical research dates back to 1940 when Schiff, Snyder and Weinberg [4] solved the Klein-Gordon equation for a square-well potential. A surprising outcome of [4] was that for strong potentials also antiparticle states become members of the bound state spectrum. For critical potential depths, i.e. the energy of particle and antiparticle states coincide, the new channel of spontaneous pair creation opens. In addition the energy eigenvalues for an electron in this short-range potential were determined in [4]. Furthermore the phenomenon of spontaneous pair creation and the transition to a charged vacuum was explored. Meanwhile numerous authors have discussed solutions of the Klein-Gordon equation for various types of strong potentials (see e.g. [5–20]).

The major intention of this work is to calculate the critical values for several long- as well as short-range potentials and to construct the corresponding eigenfunctions of the Klein-Gordon particle. A systematic comparison of solutions of this relativistic wave equation for the various types of potentials is performed. Especially we investigate the conditions necessary for antiparticle binding. The coupling strength will be always denoted by $Z\alpha$ with $\alpha = 1/137.035982$ the Sommerfeld fine structure constant. The critical number Z_{cr} is either defined by the maximum value of Z up to which the bound state solution can be obtained or by the threshold for spontaneous pair creation. In all our discussions we will stay within the framework of the single-particle interpretation of the Klein-Gordon equation. In the vicinity of critical values many-particle aspects become increasingly important. This is obvious from the following fact: Pions as the most prominent members of the Klein-Gordon family

Reprint requests to Dr. G. Soff, Gesellschaft für Schwerionenforschung mbH, Planckstraße 1, Postfach 11 05 41, D-6100 Darmstadt 11.

0340-4811 / 84 / 0800-0703 $ 01.30/0. – Please order a reprint rather than making your own copy.

obey the Bose-statistic and thus without many-particle interactions nothing could prevent the pionization of the whole universe once the critical potential depth is exceeded. For an extensive discussion of the many-particle problems we refer to [5]. In this monograph it is shown that the self-screening of spontaneously created particles prevents excessive pair creation.

In our evaluations of critical potential values we apply analytical as well as semi-analytical solutions of the Klein-Gordon differential equation. But in several cases we also make use of purely numerical techniques to obtain energy eigenvalues and eigenfunctions. This paper is organized as follows: After the introduction and some premises we briefly review the results for a spin-0 particle in the Coulomb potential of a point-like nucleus [21, 22]. Explicit expressions for the normalized wavefunctions are presented. Subsequently we investigate solutions of the equation of motion for the Coulomb potential of a finite size nucleus. It follows a treatment of a spin-0 particle in a short-range square-well potential. Here we recover the Schiff, Snyder and Weinberg [4] effect of simultaneous particle and antiparticle binding. After that we briefly present the solution for a cut-off Coulomb potential. The next sections deal with solutions for the Hulthén potential and the exponential potential. As an example we solve the Klein-Gordon equation numerically for a Yukawa potential. All types of potentials mentioned until now are considered as the fourth component of a four-vector potential.

We also couple scalar potentials of the $1/r$-type or square-well type to the Klein-Gordon equation and examine the associated solutions. Here no distinction between the behaviour of a particle and an antiparticle is possible. Finally we present a brief summary.

2. Premises

In relativistic quantum mechanics the Klein-Gordon equation describes a particle with spin 0. If we take the interaction with an electromagnetic field into account it may be represented as

$$\left[i\frac{\partial}{\partial t} - q\,A_0(\boldsymbol{r}, t)\right]^2 \Phi(\boldsymbol{r}, t) = [-i\nabla^2 - q\boldsymbol{A}(\boldsymbol{r}, t)]^2\,\Phi(\boldsymbol{r}, t) + \Phi(\boldsymbol{r}, t), \tag{2.1}$$

where q is the charge of the considered spin-0 particle and A_0 and $\boldsymbol{A}$ denote the scalar and vector part of the electromagnetic four-potential. In all our formulas we employ natural units ($\hbar = c = m = 1$). In the following we neglect the vector-potential and put $\boldsymbol{A} = 0$. Furthermore we regard only spherical symmetric and time independent potentials

$$q\,A_0(\boldsymbol{r}, t) = V(r). \tag{2.2}$$

The separation ansatz

$$\Phi(\boldsymbol{r}, t) = \Psi(\boldsymbol{r})\,e^{-iEt} \tag{2.3}$$

leads to the stationary wave equation

$$[\nabla^2 + (E - V(r))^2 - 1]\,\Psi(\boldsymbol{r}) = 0. \tag{2.4}$$

The separation of the angular part is easily performed by

$$\Psi(\boldsymbol{r}) = v(r)\,Y_{lm}(\vartheta, \varphi). \tag{2.5}$$

The radial component $v(r)$ satisfies the differential equation

$$\left[\frac{\mathrm{d}^2}{\mathrm{d}r^2} + \frac{2}{r}\frac{\mathrm{d}}{\mathrm{d}r} + k^2 - \frac{l(l+1)}{r^2}\right] v(r) = 0 \tag{2.6}$$

with

$$k^2 = (E - V(r))^2 - 1. \tag{2.7}$$

Taking

$$v(r) = u(r)/r \tag{2.8}$$

we obtain

$$\left[\frac{\mathrm{d}^2}{\mathrm{d}r^2} - \frac{l(l+1)}{r^2} + k^2\right] u(r) = 0. \tag{2.9}$$

With the substitution

$$E_S = \tfrac{1}{2}(E^2 - 1), \qquad V_S = E\,V - \tfrac{1}{2}V^2 \tag{2.10}$$

(2.9) may be cast into the form

$$\left[\frac{\mathrm{d}^2}{\mathrm{d}r^2} - \frac{l(l+1)}{r^2} + 2E_S - 2V_S(r)\right] u(r) = 0 \tag{2.11}$$

which is equivalent to the Schrödinger equation with an effective potential V_S. Furthermore with the replacement

$$y_1(r) = u(r), \qquad y_2(r) = \mathrm{d}u(r)/\mathrm{d}r \tag{2.12}$$

the second order differential equation (2.9) is readily transformed into two first order coupled differ-

ential equations

$$\frac{dy_1(r)}{dr} = y_2(r), \quad \frac{dy_2(r)}{dr} = \left[\frac{l(l+1)}{r^2} - k^2\right] y_1(r) \tag{2.13}$$

which is a proper representation for a purely numerical treatment. The radial wavefunctions are normalized according to [23, 24]

$$\int_0^\infty \varrho(r)\, r^2\, dr = \pm 1 \tag{2.14}$$

with the radial density

$$\varrho(r)\, r^2 = (E - V(r))\, u^2(r). \tag{2.15}$$

The plus-sign in (2.14) is chosen for states which enter from the upper continuum ($E > 1$) to the bound state gap with increasing coupling strength, whereas the minus-sign is taken for the antiparticle states which enter from the lower continuum ($E < -1$) to the bound state gap [14–17]. The solutions of the Klein-Gordon equation for purely scalar interactions are also normalized by the condition (2.14), but the potential in the radial density (2.15) is put to $V(r) = 0$. The chosen normalization (2.14) of the density $\varrho(r)$, which fulfills the continuity equation, also guarantees the correct nonrelativistic limit [23]. In that respect we mention that the norm of Rafelski et al. [5–7, 9] differs from ours by a factor of two.

For simplification we introduce the abbreviations

$$p = (1 - E^2)^{1/2} \tag{2.17}$$

and

$$s = 2p\, r. \tag{2.18}$$

The calculated energy eigenvalues will be given in natural units but we decided to present the radial densities ϱr^2 in units of fm^{-1}, which more or less expresses the inability of the authors to draw widespread physical conclusions from a density in natural units. For unit transformations we have used the constants $\hbar c = 197.32858$ MeV fm, $m_\pi = 139.5688$ MeV and $m_e = 0.5110034$ MeV.

3. Solution of the Klein-Gordon equation for the Coulomb potential of a point-like nucleus

The Coulomb potential is given by

$$V(r) = -Z\alpha/r, \tag{3.1}$$

where Z is the nuclear charge number and α the fine structure constant. The radial differential equation (2.9) can be solved analytically for the Coulomb potential leading to the well-known formula [21, 22] for the total energy eigenvalue

$$E = \left\{1 + \frac{(Z\alpha)^2}{(\mu + n - l - \frac{1}{2})^2}\right\}^{-1/2} \tag{3.2}$$

with $n = 1, 2, 3, \ldots$ being the principal quantum number, $l = 0, 1, 2, \ldots$ the angular quantum number. $1 - E$ is the binding energy E_b and

$$\mu = [(l + \tfrac{1}{2})^2 - (Z\alpha)^2]^{1/2}. \tag{3.3}$$

The corresponding eigenfunctions are given by

$$v(s) = N s^{\mu - \frac{1}{2}} e^{-s/2}\, {}_1F_1(-n', c; s), \tag{3.4}$$

where

$$n' = n - l - 1 \tag{3.5}$$

and

$$c = 2\mu + 1, \tag{3.6}$$

s is defined by (2.18).

The confluent hypergeometric function ${}_1F_1(-n', c; s)$ reduces to a polynomial of degree n'.

According to (2.14) the normalization constant is easily determined from

$$\frac{N^2}{(2p)^3} \int_0^\infty (E + 2pZ\alpha/s)\, s^c e^{-s}\, {}_1F_1^2(-n', c; s)\, ds = 1. \tag{3.7}$$

Employing an integration formula [25] on hypergeometric functions this yields

$$N = \left[\frac{\Gamma(c + n')}{\Gamma^2(c)\,\Gamma(n' + 1)\,(E(c + 2n') + 2pZ\alpha)}\right]^{1/2} \cdot (2p)^{3/2}. \tag{3.8}$$

From this general expression the wavefunctions of the 1s-, 2s- and 2p-state are explicitly given as

$$v_{1s}(s) = [\Gamma(c)\,(Ec + 2pZ\alpha)]^{-1/2}\,(2p)^{3/2}\, e^{-s/2}\, s^{\mu - \frac{1}{2}}, \tag{3.9a}$$

$$v_{2s}(s) = [\Gamma(c)\,(E(c + 2) + 2pZ\alpha)/c]^{-1/2}\,(2p)^{3/2} \cdot e^{-s/2}\,(s^{\mu - \frac{1}{2}} - s^{\mu + \frac{1}{2}}/c), \tag{3.9b}$$

$$v_{2p}(s) = [\Gamma(c)\,(Ec + 2pZ\alpha)]^{-1/2}\,(2p)^{3/2}\, e^{-s/2}\, s^{\mu - \frac{1}{2}}. \tag{3.9c}$$

For $Z > (l+\frac{1}{2})/\alpha$ the energy eigenvalue would take on a complex value and thus is no longer defined. The specific value $Z = (l+\frac{1}{2})/\alpha$, for which the eigenvalue still exists, is denoted as the critical charge Z_{cr}. We find $Z_{cr}(1s) = Z_{cr}(2s) \simeq 68.518$ and $Z_{cr}(2p) \simeq 205.55$.

The corresponding energy eigenvalues are immediately found to be

$$E_{1s}(Z_{cr}) = 1/\sqrt{2}, \tag{3.10a}$$

$$E_{2s}(Z_{cr}) = 3/\sqrt{10}, \tag{3.10b}$$

$$E_{2p}(Z_{cr}) = 1/\sqrt{10}. \tag{3.10c}$$

$E(Z)$ has a vertical tangent at Z_{cr}, i.e. $dE(Z_{cr})/dZ = -\infty$.

In Fig. 1 we display the energy eigenvalue of a Klein-Gordon particle in the 1s- or 2p-state bound in the Coulomb potential of a point-like nucleus with the charge number Z. For small Z the eigenvalue is close to the rest mass of the considered spin-0 particle. Contrary to a Dirac particle in a Coulomb potential the binding energy $E_b = 1 - E$ never reaches or exceeds the value $E_b = 1$ for high Z.

In Fig. 2 the radial density distribution ϱr^2 normalized according to (3.7) is plotted for a pion in the 1s-state. The chosen nuclear charge of $Z = 68$ is close to the critical value. The maximum of the radial charge density distribution is found to be at $r \simeq 0.5$ fm, the width of ϱr^2 is comparable to the Compton wavelength of a pion.

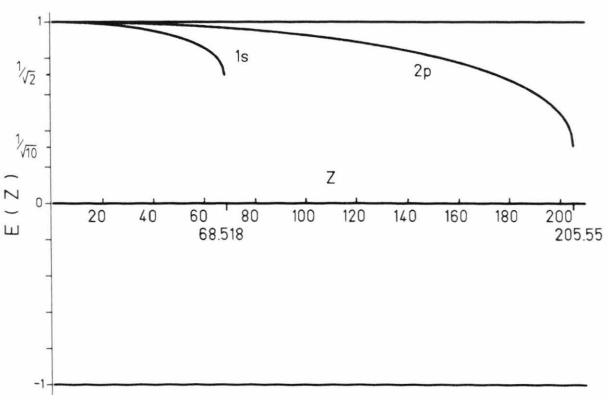

Fig. 1. The energy eigenvalue of a Klein-Gordon particle in the 1s- or 2p-state bound in the Coulomb potential of a point-like nucleus with the charge number Z. The critical nuclear charges and the corresponding eigenenergies are indicated.

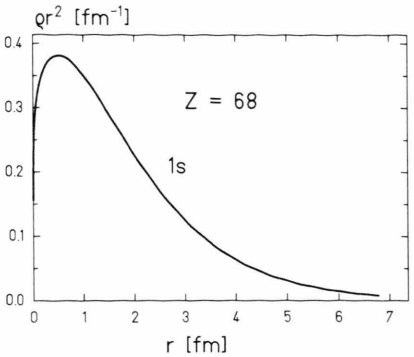

Fig. 2. The radial density distribution ϱr^2 for a pion in the 1s-state. The choosen nuclear charge $Z = 68$ is close to the critical value.

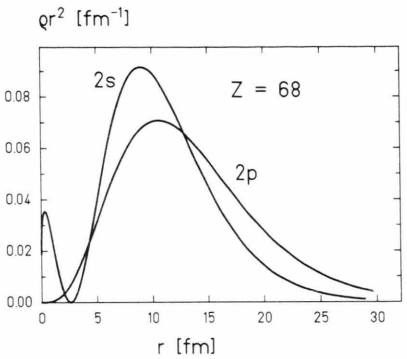

Fig. 3. The same as in Fig. 2 for the 2s- and the 2p-state, respectively.

In Fig. 3 we show the same for the 2s- and 2p-state. The 2s-wavefunction exhibits a node at $r \simeq 2.6$ fm. The almost critical nuclear charge is also reflected in the steep increase of the 1s- and 2s-radial density close to the origin $r \simeq 0$.

4. The potential of a finite size nucleus

The nuclear charge distribution is assumed to be represented by a homogeneously charged sphere of radius R. For this problem, the potential is given by

$$V(r) = \begin{cases} -\dfrac{Z\alpha}{2R}\left(3 - \dfrac{r^2}{R^2}\right), & r \leqq R, \\ -\dfrac{Z\alpha}{r}, & r > R. \end{cases} \tag{4.1}$$

Solving the radial differential equation (2.9) with this potential yields

$$u_i(r) = r^{l+1} \sum_{n=0}^{\infty} b_n r^{2n} \tag{4.2}$$

as the solution for the inner region $r \leqq R$. The coefficients are determined by

$$\begin{aligned} b_1 &= -\frac{B\, b_0}{2(2l+3)}, \\ b_2 &= -\frac{B\, b_1 - 2CA\, b_0}{4(2l+5)}, \\ b_3 &= -\frac{B\, b_2 - 2CA\, b_1 + C^2 b_0}{6(2l+7)} \end{aligned} \tag{4.3}$$

with the abbreviations

$$A = E + 3Z\alpha/(2R), \quad B = A^2 - 1, \quad C = Z\alpha/(2R^3). \tag{4.4}$$

b_0 is a normalization constant. Generally, the recurrence relation for the coefficients b_n reads

$$b_n = -\frac{B\, b_{n-1} - 2CA\, b_{n-2} + C^2 b_{n-3}}{4nl + 2n(2n+1)}. \tag{4.5}$$

For the outer region $r > R$, we obtain as solution

$$u_a(s) = N' W_{\lambda,\mu}(s) \tag{4.6}$$

which is regular for $s \to \infty$. μ is already defined by (3.3) and

$$\lambda = Z\alpha E/p. \tag{4.7}$$

The Whittacker function [20] $W_{\lambda,\mu}(s)$ can be expressed in terms of the confluent hypergeometric function via

$$\begin{aligned} W_{\lambda,\mu}(s) = &\frac{\Gamma(-2\mu)}{\Gamma(\frac{1}{2} - \mu - \lambda)} M_{\lambda,\mu}(s) \\ &+ \frac{\Gamma(2\mu)}{\Gamma(\frac{1}{2} + \mu - \lambda)} M_{\lambda,-\mu}(s) \end{aligned} \tag{4.8}$$

and

$$M_{\lambda,\mu}(s) = e^{-s/2} s^{\mu+\frac{1}{2}} {}_1F_1(\tfrac{1}{2} + \mu - \lambda, 2\mu + 1; s). \tag{4.9}$$

The energy eigenvalues are obtained from the matching condition at $r = R$

$$\frac{\frac{\mathrm{d}}{\mathrm{d}r} u_i(r)}{u_i(r)} = \frac{\frac{\mathrm{d}}{\mathrm{d}r} u_a(2pr)}{u_a(2pr)}. \tag{4.10}$$

This equation can be solved numerically by a root-finding procedure. We remark explicitly that μ can take on complex values, although the energy eigenvalue remains a real number. We determined the normalization constant b_0 such that at the matching point $r = R$ the inward solution $u_i(R)$ equals the outward solution $W_{\lambda,\mu}(2pR)$. The normalization constant prescribed by (2.14) of the total wavefunction is found numerically with a Gaussian quadrature formula [26].

A more flexible and economical approach to solve the Klein-Gordon equation is provided by the numerical integration [27] of the system of differential equations (2.13) employing predictor-corrector techniques. The initial values of y_1 and y_2 at a specific point close to $r = 0$ are computed from the power series expansion (4.2) and the relation (2.12). b_0 is still arbitrary. Taking these starting values, the integration is performed up to a matching point r_m, which for strong potentials ($E \leqq 0.5$) was placed to 3 Compton wavelengths of the bound particle. For potentials which yield a lower binding a good choice for the matching point was given by the classical turning point r_c. For s-states in a Coulomb potential it follows simply

$$r_c = Z\alpha/(1 - E). \tag{4.11}$$

In a second step the system of differential equations (2.13) is integrated from outward ($r \gg R$) to the matching point. This integration is started with

$$y_1 = c_0, \quad y_2 = -p\, y_1 \tag{4.12}$$

which can be deduced from (4.6) and (2.12) for $r \to \infty$. The arbitrary constants b_0 of the interior solution as well as c_0 in (4.12) are determined by the continuity condition of y_1 at $r = r_m$ and by the normalization condition (2.14). The radial wavefunctions left and right from the matching point are computed taking some first guess for the energy eigenvalue. Finally the energy eigenvalue is evaluated from the matching condition that also the first derivative $y_2 = \mathrm{d}u(r)/\mathrm{d}r$ must be continuous at $r = r_m$. Again a root-finding procedure may be applied to obtain the correct eigenenergy E. In Fig. 4 we show the computed radial density distribution ϱr^2 of a 1 s-pion moving in the Coulomb field of a Pb-nucleus with a radius $R = 7.0976$ fm. We compared the energy eigenvalue deduced from (4.8) with the corresponding results from the purely numerical solution of the Klein-Gordon equation

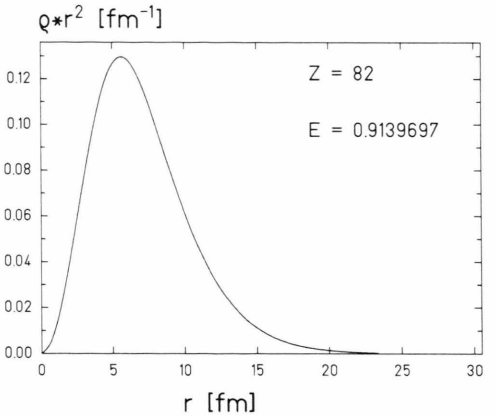

Fig. 4. The radial density distribution $\varrho\, r^2$ for a pion in the 1 s-state moving in the Coulomb potential of a Pb-nucleus ($Z = 82$) with a radius $R = 7.0976$ fm. The energy eigenvalue is indicated.

and found complete agreement. The maximum of the radial density distribution obviously is situated inside the Pb-nucleus. The width of $\varrho\, r^2$ amounts to about 3 Compton wavelengths of the pion. In the present calculations we neglected all strong interaction effects resulting from non-Coulombian forces as well as internal degrees of freedom of the pion, which limit its lifetime to about $\tau = 2.6 \times 10^{-8}$ s. The strong interaction between the nucleus and the pion causes the absorption of the orbiting particle in the nuclear matter as soon as the pionic wavefunction exhibits an overlap with the nuclear interior [28]. In consequence the energy and the radial density displayed in Fig. 4 are not observable experimentally. But similar measurements are possible for lighter elements.

To calculate the critical potential strength we increased the nuclear charge Z assuming a nuclear radius R given by

$$R = r_0 A^{1/3} \tag{4.13}$$

with $r_0 = 1.2$ fm and $A = 2.5\, Z$. The computed energy eigenvalues for the 1s- and the 2p-state are presented in Figure 5. The critical nuclear charges are $Z_{cr}(1s) = 3287$ and $Z_{cr}(2p) = 3444$, respectively. In a separate calculation we fixed the nuclear radius to $R = 10$ in natural units of the considered spin-0 particle. This reduces the critical value to $Z_{cr}(1s) = 1986$ and $Z_{cr}(2p) = 2095$, which is in complete agreement with the results derived in [6]. The corresponding energy eigenvalues as function of the nuclear charge are displayed in Figure 6. $E(Z)$ is well approximated by a straight line. The slight curvature found in Fig. 5 evidently is caused by the increasing nuclear radius $R(Z)$. For the critical nuclear $Z_{cr}(1s) = 1986$ related to the nuclear radius $R = 10\, m_\pi^{-1} \simeq 14.1384$ fm we plot in Fig. 7 the radial density distribution of a pion in the 1s-state. It looks similar to $\varrho\, r^2$ for pionic lead. A noticeable difference not visible in the figure follows from the fact that for $E < 0$ the density ϱ takes on negative values for $r > -Z\alpha/E$.

The radial density $\varrho\, r^2$ in fm^{-1} for a Klein-Gordon particle (solid line) with the mass m_e of an electron in the Coulomb field of a finite size nucleus is depicted in Figure 8. For comparison the dashed line shows the same for an electron in the $1s_{1/2}$-state computed [29] within the framework of the Dirac

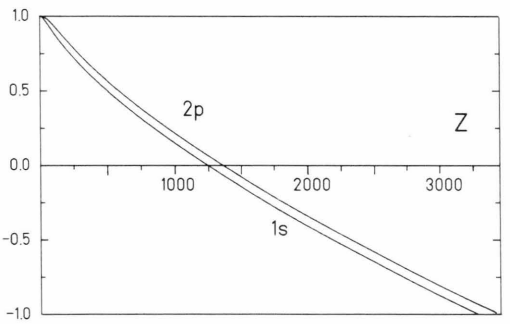

Fig. 5. The energy eigenvalue $E(Z)$ of a pion in the 1s-state and 2p-state, respectively. The potential is determined by a homogeneously charged sphere of radius $R = r_0 A^{1/3}$ with $r_0 = 1.2$ fm and $A = 2.5\, Z$. The critical nuclear charges are $Z_{cr}(1s) = 3287$ and $Z_{cr}(2p) = 3444$, respectively.

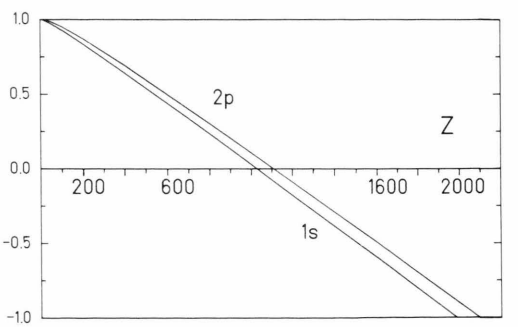

Fig. 6. The same as in Fig. 5 for a fixed nuclear radius $R = 10$ in natural units (Compton wavelength of the considered spin-0 particle). The critical nuclear charges are $Z_{cr}(1s) = 1986$ and $Z_{cr} = 2095$, respectively.

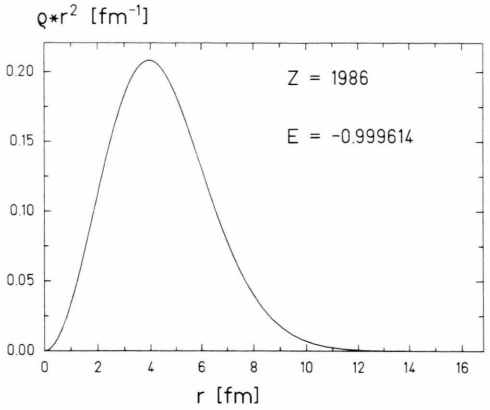

Fig. 7. The radial density distribution $\varrho\, r^2$ of a pion in the 1s-state for the critical nuclear charge $Z = 1986$. Not visible on a linear scale is the negative density for $r > Z\,\alpha \sim 20.5$ fm due to the exponential decline of $\varrho\, r^2$ for large r.

equation. The nuclear charge numbers $Z = 30$ and $Z = 107$ are considered, the latter coincides with the critical value for the spin-0 particle. For $Z = 30$ both densities still look very similar, whereas for $Z = 107$ considerable differences appear. Most striking is the sharp localization of the Klein-Gordon density close to the origin.

5. The square-well potential

The potential simply reads

$$V(r) = -V_0\,\theta\,(R - r), \tag{5.1}$$

where $\theta\,(x)$ denotes the Heaviside unit step function. Starting from the differential equation (2.6) for the radial function v we obtain as solution for $r \leqq R$

$$v_{\mathrm{i}}\,(k_{\mathrm{i}}\,r) = N\,j_l\,(k_{\mathrm{i}}\,r) \tag{5.2}$$

with (cf. (2.7))

$$k_{\mathrm{i}}^2 = (E + V_0)^2 - 1, \tag{5.3}$$

$l = 0, 1, 2, \ldots$ is the angular momentum quantum number. N is a normalization constant. $j_l\,(k_{\mathrm{i}}\,r)$ signifies the spherical Bessel-function [26], which is regular for $r \to 0$. It can be expressed explicitly for $l = 0,1$ as follows [26]:

$$j_0\,(k_{\mathrm{i}}\,r) = \sin\,(k_{\mathrm{i}}\,r)/k_{\mathrm{i}}\,r \tag{5.4a}$$

$$j_1\,(k_{\mathrm{i}}\,r) = \sin\,(k_{\mathrm{i}}\,r)/(k_{\mathrm{i}}\,r)^2 - \cos\,(k_{\mathrm{i}}\,r)/k_{\mathrm{i}}\,r\,. \tag{5.4b}$$

For the outer region $r > R$, the solution is given by

$$v_{\mathrm{a}}\,(i\,k_{\mathrm{a}}\,r) = N'\,h_l^{(1)}\,(i\,k_{\mathrm{a}}\,r) \tag{5.5}$$

with

$$k_{\mathrm{a}}^2 = p^2. \tag{5.6}$$

N' again is a normalization constant. $h_l^{(1)}\,(i\,k_{\mathrm{a}}\,r)$ denotes the Hankel-function [26], which is regular at

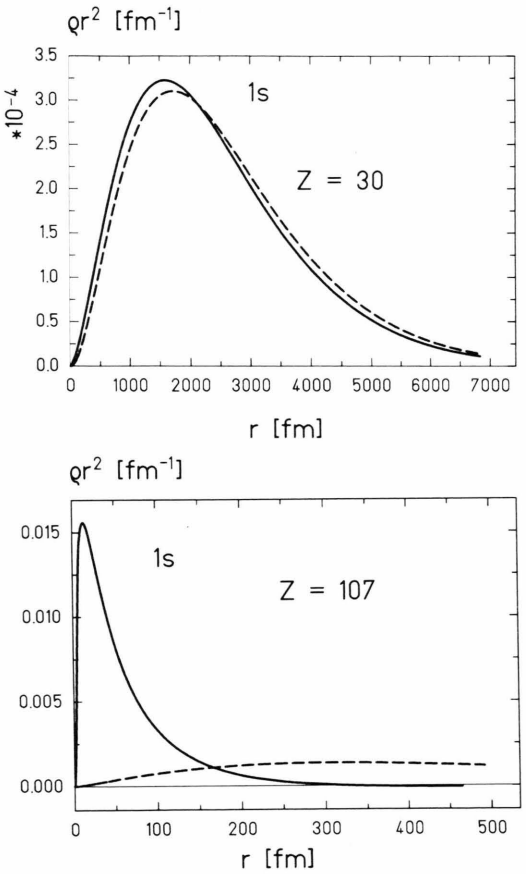

Fig. 8. The radial density $\varrho\, r^2$ in fm^{-1} for a Klein-Gordon particle (solid line) with the mass of an electron in the Coulomb field of a finite size nucleus. The nuclear radius was determined via $R = r_0 A^{1/3}$ with $r_0 = 1.2$ fm and $A = 2.5\,Z$. For comparison the dashed line shows the radial density of an electron in the $1\,s_{1/2}$-state computed within the framework of the Dirac equation. a) For the nuclear charge number $Z = 30$ both densities look quite similar, which also underlines the correct normalization of the Klein-Gordon wavefunction. The corresponding energy eigenvalues are for the Klein-Gordon particle $E\,(1s) = 0.974451$ and for the Dirac particle $E\,(1s_{1/2}) = 0.975743$, respectively. b) The same as in a) for the critical nuclear charge number $Z = 107$. The Klein-Gordon density is sharply localized close to the nucleus whereas the Dirac density still exhibits a broad distribution. We obtained $E\,(1s) = -0.896356$ and $E\,(1s_{1/2}) = 0.626661$.

infinity. For $l = 0,1$ it can be written as [26]

$$h_0^{(1)}(i\,k_a\,r) = -1/(k_a\,r)\exp(-k_a\,r) \tag{5.7a}$$

$$h_1^{(1)}(i\,k_a\,r) = i\left[\frac{1}{k_a\,r} + \frac{1}{(k_a\,r)^2}\right]\exp(-k_a\,r). \tag{5.7b}$$

Again, the energy eigenvalue will be found by the matching procedure

$$\frac{\frac{\mathrm{d}}{\mathrm{d}r}v_i(k_i\,r)}{v_i(k_i\,r)} = \frac{\frac{\mathrm{d}}{\mathrm{d}r}v_a(i\,k_a\,r)}{v_a(i\,k_a\,r)} \tag{5.8}$$

at $r = R$, which for the lowest angular momentum state ($l = 0$) leads to

$$\tan(k_i\,R) = -k_i/k_a \tag{5.9}$$

whereas for $l = 1$ we found

$$(1 - \xi\cot\xi)/\xi^2 = -(1+\eta)/\eta^2 \tag{5.10}$$

with $\eta = k_a\,R$ and $\xi = k_i\,R$. The normalization constant in general is determined by (2.14). For $l = 0$ N is explicitly given by

$$N = \sqrt{2}\,k_i\,[(E+V_0)\,(R - \tfrac{1}{2}\sin(2\,k_i\,R)/k_i) + E\sin^2(k_i\,R)/k_a]^{-1/2} \tag{5.11}$$

and N' is determined by $N' = N\,j_l(k_i\,R)/h_l^{(1)}(i\,k_a\,R)$.

In Fig. 9 we present as a function of the coupling strength parameter Z the energy eigenvalue of a pion, which occupies the 1s-state in a square-well potential. The potential depth is determined by

$$V_0 = Z\,\alpha/R \tag{5.12}$$

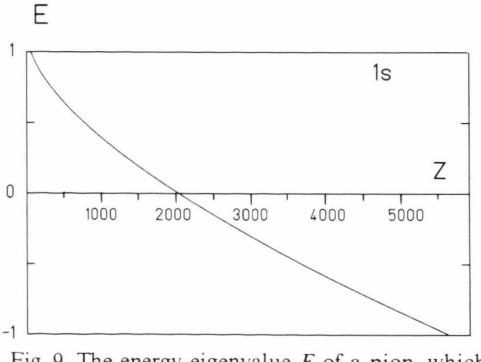

Fig. 9. The energy eigenvalue E of a pion, which occupies the 1s-state in a square-well potential. The potential depth follows from (5.12) and (5.13). Not visible on this scale is the simultaneous existence of two solutions for $Z = 5624$ and 5625.

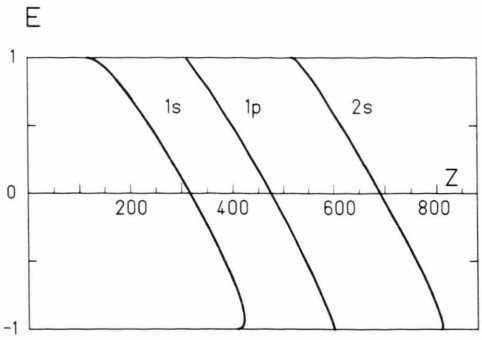

Fig. 10. The energy eigenvalue E of a pion in a square-well potential. E is plotted versus Z for the 1s-, 1p- and 2s-state, respectively. The potential depth follows from $V_0 = -Z\,\alpha/R$ with a fixed radius of $R = 1.5$ fm. At $E \simeq -1$ the existence of two solutions for a fixed Z becomes visible for the 1s-state as well as for the 2s-state.

for $r \leqq R$. The radius R was assumed to depend on Z via

$$R = r_0\,(2.5\,Z)^{1/3} \tag{5.13}$$

with $r_0 = 1.2$ fm. The energy eigenvalue decreases monotonically until $Z = 5623$. For $Z = 5624$ and $Z = 5625$ we found two solutions of the transcendental equation (5.9) corresponding to particle and antiparticle binding, respectively [4]. Thus for this type of potential the critical value $Z_{cr}(1s) = 5626$ is not fixed by the condition that the energy eigenvalue E reaches the value $E = -1$, but rather by the energetical coincidence of the particle and antiparticle bound state. A similar phenomenon for the 1p-state could not be found. At $Z = 5659$ we obtained from (5.10) $E(1p) = -1$.

To explore in more detail the Schiff, Snyder, Weinberg effect [4] we fixed in an additional calculation the radius R of the potential domain to a small value of $R = 1.5$ fm, which roughly corresponds to the Compton wavelength of a pion ($\lambda\!\!\!^{-}_{\pi} \sim 1.41$ fm).

The computed energy eigenvalues of the 1s-, 1p- and 2s-state, respectively are plotted in Fig. 10 versus the coupling strength parameter Z. The simultaneous existence of two values of E for a fixed Z becomes visible for the 1s-state as well as for the 2s-state at $E \sim -1$. At $Z = 406$ the antiparticle 1s-state enters the bound state gap ($1 > E > -1$). The critical value, where the energy of the particle and antiparticle state coincides is found to be $Z_{cr}(1s) =$

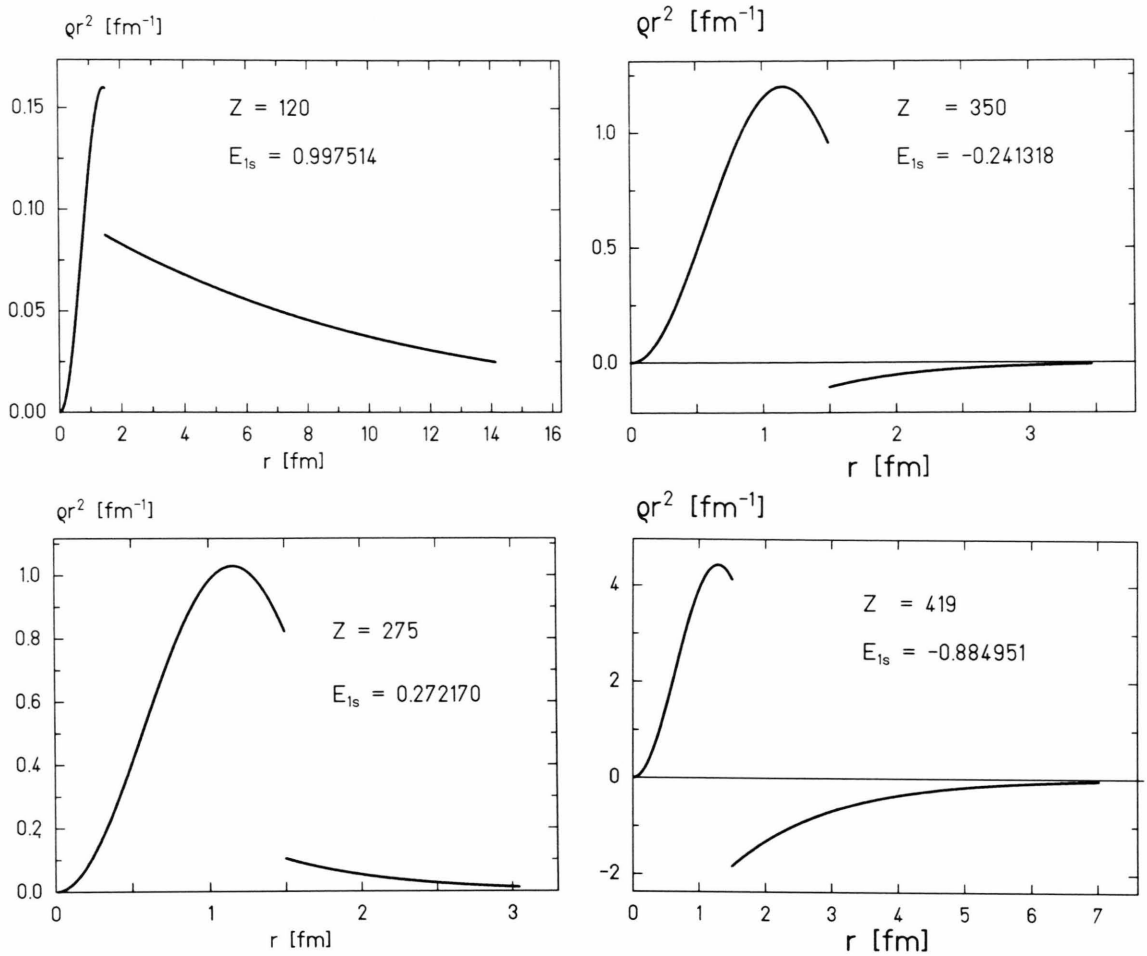

Fig. 11. The radial density distribution ϱr^2 in fm^{-1} of a pion, which occupies the 1s-state in a square-well potential. The radius R of the potential well was fixed to $R = 1.5$ fm. Different coupling strength parameters Z are considered. The related energy eigenvalues E_{1s} are indicated. Please, note the different scales. ϱr^2 displays a discontinuity at $r = R$. For negative values of E also the radial density ϱr^2 gets negative outside the attractive potential ($r > R$).

420. The corresponding numbers for the 2s-state are $Z(E_{2s} = -1) = 808$ and $Z_{cr}(2s) = 810$.

Again the centrifugal barrier seems to hinder the equivalent phenomenon for states with angular momenta different from $l = 0$. No inflection point in $E_{1p}(Z)$ is found. We get $E_{1p} \simeq -1$ at $Z = 599$.

A more profound insight allows the consideration of the radial charge density ϱr^2, which is presented in Fig. 11 for the 1s-state and various values of Z. Most striking is the discontinuity of ϱ at $r = R$, which can be traced back to the factor $(E - V(r))$ in (2.15) and to the discontinuity of the square-well potential. For negative values of E also the radial density ϱr^2 gets negative outside the attractive potential ($r > R$). Obviously, the conventional interpretation of ϱ as the position probability density of a single spin-0 particle completely breaks down at this point. For strong potentials the Klein-Gordon equation inherently enforces the implementation of many-particle aspects. The density distribution ϱr^2 is sharply localized, i.e. the width is of the order of $\lambda\!\!\!^{-}_{\pi}$, as soon as the binding energy is comparable to the rest mass of the bound particle. In Fig. 12 we investigate the radial charge density ϱr^2 of the antiparticle (dashed line) for $Z = 407$ and $Z = 418$, respectively. In contrast to the particle state, which is

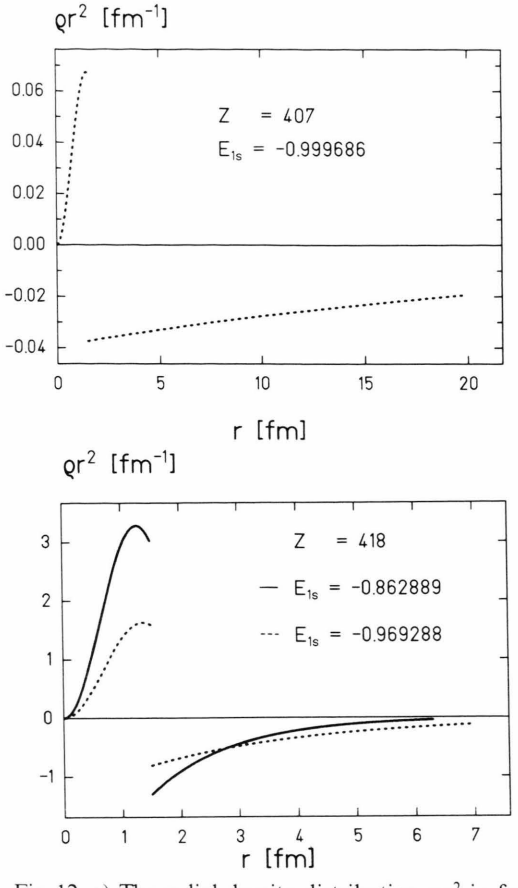

Fig. 12. a) The radial density distribution ϱr^2 in fm^{-1} for the antiparticle bound state in a square-well potential with a fixed radius $R = 1.5$ fm. Z has been chosen such that the binding energy of the antiparticle yields a small value compared to its rest mass. The low binding energy is also reflected in the widespread radial distribution, which obviously is much broader than the Compton wavelength of a pion. b) Comparison of the radial density distribution of a $\pi^- \rightarrow$ particle (solid line) and a $\pi^+ \rightarrow$ an antiparticle (dashed line) in a square-well potential with a fixed radius $R = 1.5$ fm. The corresponding energy eigenvalues E_{1s} are indicated. The particle state is normalized to 1 according to (2.11). The antiparticle state is normalized to -1, i.e. the norm is determined by the radial density outside the potential well ($r > R$).

normalized to 1 according to (2.14), the antiparticle state is normalized [14–17] to -1, i.e. the norm is dominated by the radial density outside the potential well ($r > R$). ϱr^2 in Fig. 12b looks similar for both states. The corresponding wavefunctions exhibit almost a complete overlap. Therefore the simultaneous binding of a particle and an antiparticle inevitably necessitates to take into account the mutual interaction between both pions.

In conclusion we have recovered the fact that due to relativistic effects also an antiparticle may be bound in a sufficiently strong potential, which conventionally is repulsive for that meson. In this case the particle component of the charge density, which is located inside the potential well, causes the binding.

In Fig. 13 we display the same as in Fig. 12b for the 2s-state at $Z = 810$. It is interesting to note, that the node of the radial wavefunction is located inside the well both for the particle (solid line) and the antiparticle state (dashed line).

6. The cut-off Coulomb potential

For $r > R$, the potential is identical with the ordinary Coulomb potential of a point-like nucleus. For $r \leqq R$, the potential is assumed to be constant. Thus it follows

$$V(r) = \begin{cases} -Z\alpha/R, & r \leqq R, \\ -Z\alpha/r, & r > R. \end{cases} \tag{6.1}$$

This corresponds to the Coulomb potential of a spherical shell with radius R and with the charge number Z.

As in Chapt. 4 the solution for $r > R$ is specified by

$$v_a(2pr) = N' W_{\lambda,\mu}(2pr)/r. \tag{6.2}$$

The solution for the inner region is the same as for the square-well potential (preceding chapter)

$$v_i(k_i r) = N j_l(k_i r). \tag{6.3}$$

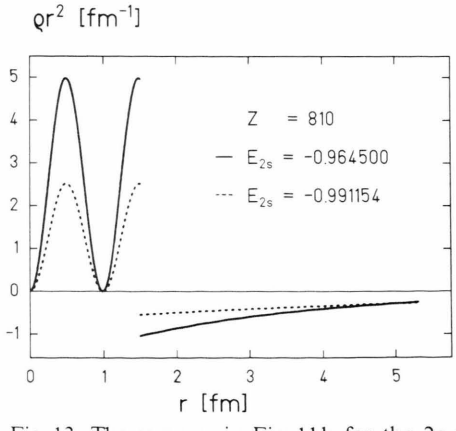

Fig. 13. The same as in Fig. 11b for the 2s-state at $Z = 810$. The node of the radial wavefunction is located inside the square well potential.

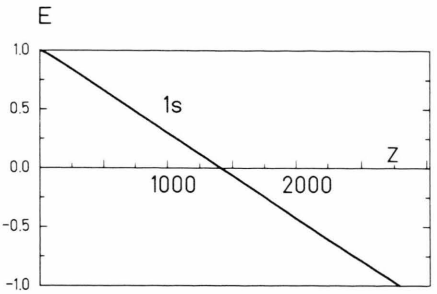

Fig. 14. The energy eigenvalue E of a pion, which occupies the 1s-state in a cut-off Coulomb potential. The radius R of the spherical shell with charge number Z was fixed to $R = 10$. The critical value is $Z_{cr}(1s) = 2786$.

The total radial wavefunction then reads

$$v(r) = v_i(k_i r)\,\theta(R - r) + v_a(2 p r)\,\theta(r - R). \tag{6.4}$$

The matching condition, from which we get the energy eigenvalues, reads here

$$\frac{\frac{d}{dr} j_l(k_i r)}{j_l(k_i r)} = \frac{\frac{d}{dr}[W_{\lambda,\mu}(2 p r)/r]}{W_{\lambda,\mu}(2 p r)/r} \tag{6.5}$$

at $r = R$. The normalization constant is determined numerically from the general condition (2.14).

In Fig. 14 we show the energy eigenvalue E of a pion, which occupies the 1s-state in the cut-off Coulomb potential. The radius R of the spherical shell was fixed to $R = 10$. E_{1s} displays a linear dependence on the charge number Z. The critical value is $Z_{cr}(1s) = 2786$. No antiparticle bound state was found.

7. The Hulthén potential

In this chapter we discuss again the behaviour of a spin-0 particle in a short-range potential $V(r)$, which is coupled as the forth component of a four-vector to the Klein-Gordon equation. The Hulthén potential reads

$$V(r) = -Z\alpha \frac{\exp(-r/a)}{1 - \exp(-r/a)}. \tag{7.1}$$

This potential is graphically represented in Fig. 15 for $Z\alpha = 1$ and $a = 1$. The dependence on the radial coordinate r is compared with the exponential potential and the Yukawa potential, which will be treated in Chapt. 8 and 9, respectively. Obviously, the Hulthén potential exhibits an exponential decline for $r \gg a$ and behaves like $1/r$ for $0 < r \ll a$. From the latter fact we already expect that the critical values for the coupling strength parameters Z are similar to those for the Coulomb potential. In Chapt. 3 we found that Z_{cr} was determined from the requirement of a regular radial density $\varrho\, r^2$ at $r \sim 0$.

For s-states ($l = 0$) the Klein-Gordon equation with a Hulthén potential can be solved analytically. This was first demonstrated by Calucci and Ghirardi [10]. In the following studies we thus consider predominantly this specific angular momentum state. We start from (2.7) and (2.9) and make the separation ansatz

$$u(r) = \exp(-p r)\,(1 - \exp(-r/a))^{\lambda+1}\, w(r); \tag{7.2}$$

p is given by the definition (2.17) and λ follows from the substitution

$$\lambda(\lambda + 1) = -(Z\alpha)^2 a^2 \tag{7.3}$$

which yields

$$\lambda = -\tfrac{1}{2} + \{\tfrac{1}{4} - (Z\alpha)^2 a^2\}^{1/2}. \tag{7.4}$$

The parameter λ determines the behaviour of the wavefunction close to the origin. From the constraint to obtain a regular bound state wavefunction we conclude that λ should be real and greater than $-\frac{1}{2}$. This already determines the critical value for s-states. From (7.4) we derive

$$Z_{cr} = 1/(2\alpha a). \tag{7.5}$$

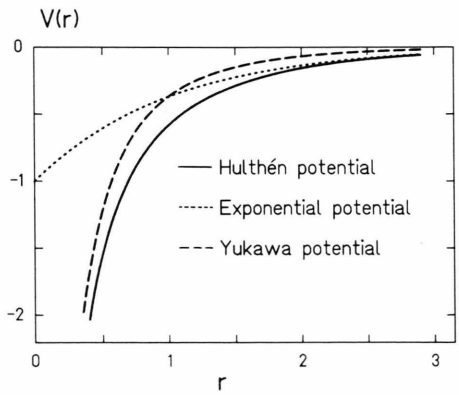

Fig. 15. Graphical representation of the Hulthén potential, the exponential potential and the Yukawa potential. Natural units are employed. In each case the fall-off constant was fixed to $a = 1$. The coupling strength was chosen to be $Z\alpha = 1$.

For $a=1$ this coincides with the corresponding result for the Coulomb potential. Taking the ansatz (7.2) and the substitution

$$t=1-\exp(-r/a) \tag{7.6}$$

we arrive at

$$t(1-t)\frac{\mathrm{d}^2 w}{\mathrm{d}t^2}+\{2(\lambda+1)-(3+2\lambda+2p\,a)\,t\}\frac{\mathrm{d}w}{\mathrm{d}t}$$
$$+\{2EZ\alpha a^2-(\lambda+1)(1+2p\,a)\}w=0. \tag{7.7}$$

This is the differential equation defining the hypergeometric function ${}_2F_1(a', b; c; t)$ [26]. Hence the total radial wavefunction may be written as

$$u(r)=N\exp(-p\,r)(1-\exp(-r/a))^{\lambda+1}$$
$$\cdot\,{}_2F_1(a', b; c; 1-\exp(-r/a)). \tag{7.8}$$

Here we have employed the abbreviations

$$a'=\lambda+1+p\,a-\{\lambda(\lambda+1)+p^2a^2+2Z\alpha E a^2\}^{1/2},$$
$$b=\lambda+1+p\,a+\{\lambda(\lambda+1)+p^2a^2+2Z\alpha E a^2\}^{1/2},$$
$$c=2(\lambda+1). \tag{7.9}$$

With a well-known transformation formula [26] for the hypergeometric function the radial wavefunction may be represented as

$$u(r)=N(1-\exp(-r/a))^{\lambda+1}$$
$$\cdot\left\{\frac{\Gamma(c)\Gamma(c-a'-b)}{\Gamma(c-a')\Gamma(c-b)}\,{}_2F_1(a', b; a'+b-c+1; \exp(-r/a))\exp(-p\,r)\right.$$
$$\left.+\frac{\Gamma(c)\Gamma(a'+b-c)}{\Gamma(a')\Gamma(b)}\,{}_2F_1(c-a', c-b; c-a'-b+1; \exp(-r/a))\exp(p\,r)\right\}. \tag{7.10}$$

Due to the exponential factor the second term in (7.10) is divergent for $r\to\infty$. In order to allow for normalizable bound states the prefactor of this second term must vanish, i.e.

$$\frac{\Gamma(c)\Gamma(a'+b-c)}{\Gamma(a')\Gamma(b)}=0. \tag{7.11}$$

This equation holds if

$$(n_r+a')(n_r+b)=0 \tag{7.12}$$

with

$$n_r=0, 1, 2, \ldots . \tag{7.13}$$

With the definition

$$n=n_r+1 \tag{7.14}$$

it follows from (7.12) and (7.9)

$$2EZ\alpha a^2+\lambda(\lambda+1)-2p\,a(n+\lambda)-(n+\lambda)^2=0. \tag{7.15}$$

As the next step we investigate the necessary conditions for the formation of a bound state. Taking the simple fact that at the threshold to the upper continuum the momentum vanishes ($E=1$, $p=0$) we find immediately

$$(n+\lambda)^2+(Z\alpha)^2a^2<2Z\alpha a^2. \tag{7.16}$$

This inequality implies a condition both on the coupling strength and on the range of the potential. The first bound state, which enters the gap $-1\leqq E\leqq 1$, trivially is characterized by the quantum number $n=1$. In addition we employ the definition (7.4) for λ, which yields with the relation (7.16)

$$\frac{2}{1+4a^2}<Z\alpha<\frac{1}{2a}. \tag{7.17}$$

The right-hand part stems from relation (7.5). For the special case $a=1$ we deduce from (7.17) that the coupling strength is restricted to a rather narrow domain of $2/5<Z\alpha<1/2$. If we insert the maximum value of $Z\alpha$ into (7.16) it follows

$$a>\tfrac{1}{2}. \tag{7.18}$$

The relation (7.16) furthermore provides a constraint on the quantum number n. Solving the corresponding quadratic equation we get

$$1\leqq n<-\lambda+a\{2Z\alpha-(Z\alpha)^2\}^{1/2}. \tag{7.19}$$

Once these conditions are fulfilled one can evaluate the energy eigenvalue E from (7.15). After some elementary transformations we obtain for the bound states with angular momenta $l=0$

$$E=\frac{Z\alpha}{2}+\frac{n+\lambda}{2a}\left\{\frac{4a^2}{(n+\lambda)^2+(Z\alpha)^2a^2}-1\right\}^{1/2}. \tag{7.20}$$

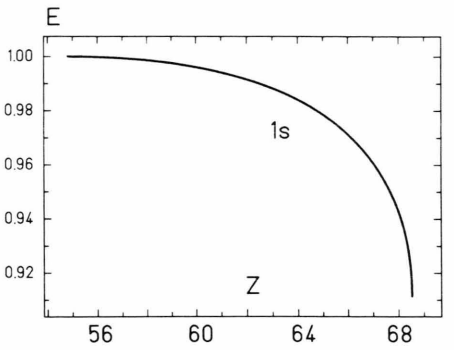

Fig. 16. The energy eigenvalue E of a Klein-Gordon particle in a Hulthén potential with a fall-off constant $a = 1$. E is plotted for the 1s-state as a function of the coupling strength parameter Z. At the critical value $Z_{cr} = 1/(2\alpha)$ it follows $E(Z_{cr}) = (1+\sqrt{7})/4$.

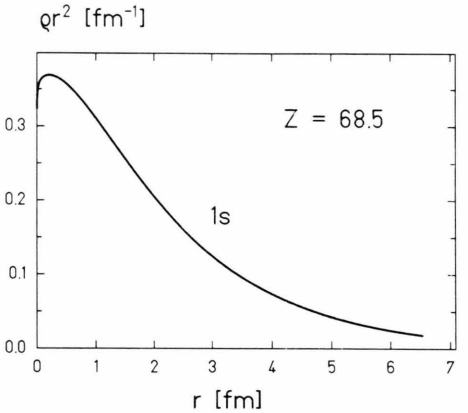

Fig. 17. The radial density ϱr^2 of a pion in a Hulthén potential with a fall-off constant $a = 1$. The chosen coupling strength parameter $Z = 68.5$ is close to the critical value of $Z_{cr} = 1/(2\alpha)$. The maximum of the radial density for the 1s-state is situated close to the origin at $r \sim 0$.

For $Z = Z_{cr}$ and $a = 1$ this leads to $E(Z_{cr}) = (1+\sqrt{7})/4$ and to $dE(Z_{cr})/dZ = -\infty$. The singular potential obviously prevents the appearence of an antiparticle bound state. In Fig. 16 the energy eigenvalue E is plotted for $n = 1$. Please note the modified scale compared with previous figures caused by the rather narrow domain for $Z\alpha$. $E(Z)$ displays the square root dependence according to (7.20).

The normalization constant N of the radial wavefunction (7.8) or (7.10) was determined numerically according to (2.14). The radial density ϱr^2 of a pion in a Hulthén potential with a fall-off constant $a = 1$ is presented in Figure 17. The chosen coupling strength parameter $Z = 68.5$ is close to the critical value $Z_{cr} = 1/(2\alpha)$. The criticality is also reflected in the fact, that the maximum of the 1s-radial density is situated near the origin at $r \sim 0$.

Numerically we determined also bound states with angular momenta $l = 1$. But for $a = 1$ bound states were found only for an extremely narrow domain of $Z\alpha$, i.e. Z could be at most half a unit smaller than the critical value of $Z_{cr}(2\,p) = 3/(2\alpha) \simeq 205.55$. For this reason we renounced to plot $E_{2p}(Z)$.

8. The exponential potential

The exponential potential has the simple form

$$V(r) = -Z\alpha \exp(-r/a). \tag{8.1}$$

The dependence on the radial coordinate is depicted in Fig. 15 for $Z\alpha = 1$ and $a = 1$. It is important to note that the exponential potential is regular at the origin in contrast to the Hulthén potential and the Yukawa potential, respectively. Bawin and Lavine [11] demonstrated that the Klein-Gordon equation with the potential (8.1) can be solved analytically for s-waves. Therefore we also specify our investigations to s-states ($l = 0$). We start with the separation ansatz

$$u(r) = \exp\{r/(2a)\}\, w(t) \tag{8.2}$$

and the substitution

$$t = 2i Z\alpha a \exp(-r/a). \tag{8.3}$$

The insertion of this ansatz and the potential (8.1) into (2.7) leads to

$$\frac{d^2 w}{dt^2} + [-\tfrac{1}{4} - iEa/t + (\tfrac{1}{4} - p^2 a^2)/t^2]\, w = 0. \tag{8.4}$$

This is just the Whittacker differential equation [26]. The solution which is bounded at $r \to \infty$, i.e. $t = 0$ is given by

$$w(t) = N M_{\lambda,\mu}(t) \tag{8.5}$$
$$= N e^{-t/2} t^{\frac{1}{2}+\mu}\, {}_1F_1(\tfrac{1}{2} + \mu - \lambda, 1 + 2\mu; t)$$

with

$$\lambda = -iEa, \quad \mu = pa. \tag{8.6}$$

The total radial wavefunction thus reads

$$u(r) = N \exp\{r/(2a)\}\, M_{\lambda,\mu}(2i Z\alpha a \exp(-r/a)). \tag{8.7}$$

The bound-state spectrum follows from the requirement that $u(r)$ vanishes at $r = 0$, which yields

$$ {}_1F_1\left(\tfrac{1}{2} + \mu - \lambda, 1 + 2\mu; 2i Z \alpha a\right) = 0. \qquad (8.8) $$

This implicit equation determines the energy eigenvalues for s-states. The normalization factor N in (8.5) and (8.7) is computed numerically according to the condition (2.14).

The calculated energy eigenvalues E of a pion in an exponential potential are plotted in Fig. 18 versus the coupling strength parameter Z. Only the strongest bound s-state is considered. The fall-off constant in the potential (8.1) was fixed to $a = 1$. At $Z_{cr} \simeq 778$ the 1s-state reaches the boundary ($E = -1$) to the negative energy continuum. The range of the potential was still too far to yield an antiparticle bound state in our numerical studies. In a second calculation we lowered the fall-off constant to $a = 0.2$. This causes an increase of the critical value to $Z_{cr} \simeq 2158$, which can be taken from Figure 19. In addition we now obtained also an antiparticle bound state for $2150 < Z < 2158$. The related energies may be deduced from the dashed line in the inset of Figure 19. The occurrence of this antiparticle bound state thus is not directly correlated with a discontinuity of the potential but rather with the range of the interaction. In Fig. 20 we show the radial density ϱr^2 of a pion for $a = 0.2$ and the almost critical value $Z = 2158$. ϱr^2 for the antiparticle bound state is displayed by the dashed line. The corresponding energy eigenvalues are given explicitly. A striking feature is the rather high density at $r \simeq 0.3$ fm compared with similar results for long-range potentials. It is easy to verify, that the analytical treatment of Bawin and Lavine [11] is correct. However, we have to emphasize, that we were not able to reproduce the numerical results for $E(Z\alpha)$ presented in the figures of [11]. To check our results we compared our analytical evaluations with the outcome of a purely numerical solution of the Klein-Gordon equation with an exponential potential. Within the numerical accuracy total agreement was achieved.

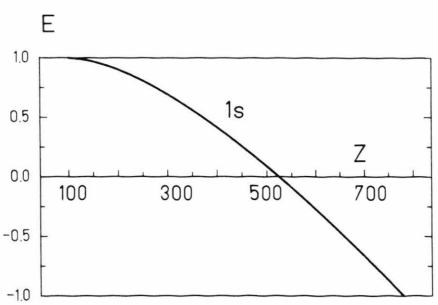

Fig. 18. The energy eigenvalue of a pion in an exponential potential versus the coupling strength parameter Z. The fall-off constant was chosen to be $a = 1$. Only the 1s-state is considered. No antiparticle bound state could be detected. $Z_{cr} \simeq 778$.

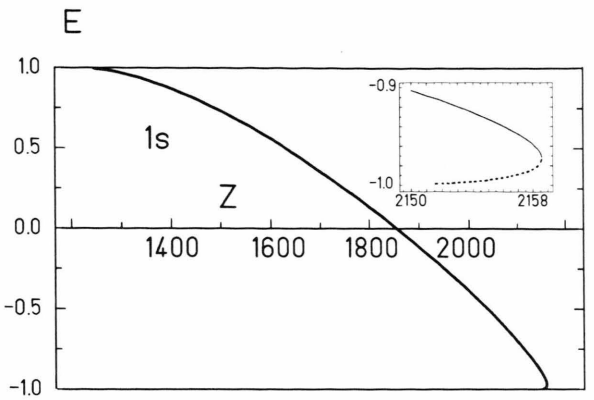

Fig. 19. The same as in Fig. 18 for $a = 0.2$. Also energy eigenvalues E for antiparticle bound states were computed. $Z_{cr} \simeq 2158$. The inset displays E in the domain $2150 \leqq Z \leqq 2158$. The dashed line indicates E for the antiparticle state.

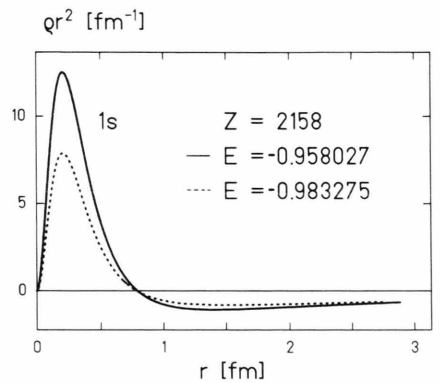

Fig. 20. The radial density ϱr^2 of a π-meson, which occupies the 1s-state in an exponential potential. The fall-off constant was chosen to be $a = 0.2$, the coupling strength parameter is $Z = 2158$. The dashed line denotes ϱr^2 for the antiparticle bound state. The corresponding energy eigenvalues are indicated. A striking feature is the rather high magnitude of ϱr^2 at $r \simeq 0.3$ fm compared with related densities for long-range potentials.

9. The Yukawa potential

The Yukawa potential

$$V(r) = -Z\,\alpha \exp(-r/a)/r \tag{9.1}$$

displays the same type of singularity at the origin as the Coulomb potential of a point-like nucleus or the Hulthén potential. Its spatial distribution is represented in Figure 15. We solved numerically (2.9) with the potential (9.1) starting with the initial values for $r \ll a$

$$u = \text{const}, \quad \frac{du}{dr} = (\mu + \tfrac{1}{2})\,u/r \tag{9.2}$$

with μ taken from the definition (3.3). The energy eigenvalues E are computed with the methods as described in Chapter 4. For a fall-off constant $a = 1$ we could identify bound states only for the rather small range $(Z_{cr} - Z) < 1$ with

$$Z_{cr} = 1/(2\,\alpha). \tag{9.3}$$

For the 1s-state and $a = 2$ the energy eigenvalue is presented in Figure 21. E exhibits a similar dependence on Z as the energies obtained for the Hulthén potential.

10. The scalar $1/r$-potential

Now we start the investigations from the differential equation

$$\left[\frac{d^2}{dr^2} - \frac{l(l+1)}{r^2} + E^2 - 1 - W(r)\right] u(r) = 0. \tag{10.1}$$

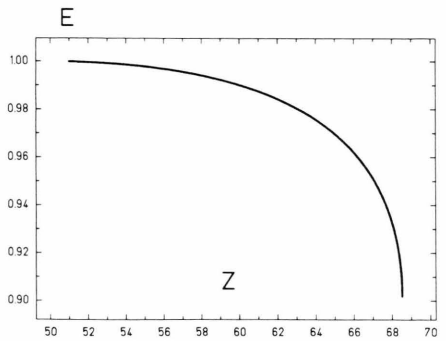

Fig. 21. The energy eigenvalue E of a pion in a Yukawa potential with a fall-off constant $a = 2$. E is presented for the 1s-state. The critical coupling strength parameter is $Z_{cr} = 1/(2\,\alpha)$.

As a first example we consider the long-range scalar potential

$$W(r) = -Z\,\alpha/r. \tag{10.2}$$

Again α denotes the fine-structure constant and Z determines the coupling strength. Please note, that the scalar potential in (10.1) is not directly coupled to the mass but rather to the square of the mass $(m^2 = 1)$. One should also stress that a scalar potential as in (10.2) obviously is of no relevance in physical measurements. There is no experimental evidence for such a long-range interaction, which is independent of the charge of the spin-0 particle and which in consequence does not distinguish between particles and antiparticles. Nonetheless, we think that it is interesting to exploit the formal solution of the Klein-Gordon equation for this unusual type of potential and to calculate the critical values for pair creation.

With the substitutions (2.17) and (2.18) Eq. (7.1) takes a form which is similar to the Schrödinger equation for the hydrogen problem. Following the way of solving the Schrödinger equation for hydrogen-like atoms we find immediately

$$E = \pm\left[1 - \frac{(Z\,\alpha)^2}{4n^2}\right]^{1/2}. \tag{10.3}$$

Here, again, n denotes the principal quantum number, which is related to the radial quantum number n_r and the angular momentum quantum number l via

$$n = n_r + l + 1. \tag{10.4}$$

As for the non-relativistic wave equation the energy eigenvalue E is independent of the angular momentum quantum number l. As expected, E is symmetric for particle and antiparticle states, respectively. The critical values are easily found to be

$$Z_{cr} = 2n/\alpha \tag{10.5}$$

which explicitly yields $Z_{cr}(1s) \simeq 274.07$ and $Z_{cr}(2s) = Z_{cr}(2p) \simeq 548.14$. Evidently, it follows $dE(Z_{cr})/dZ = \pm\infty$. The radial wavefunctions are given by

$$v(s) = N\,s^l\,{}_1F_1(-n + l + 1, 2l + 2, s)\,e^{-s/2}; \tag{10.6}$$

$v(s)$ may be also expressed in terms of generalized Laguerre polynomials [26]

$$v(s) = N\,s^l\,\frac{(n-l-1)!}{(n+l)!}\,(2l+1)!\,L_{n-l-1}^{(2l+1)}(s)\,e^{-s/2}. \tag{10.7}$$

The normalization constant N follows from (2.14) with $V(r) = 0$. This leads to

$$N = \sqrt{\frac{(n+l)!}{2\,|E|\,n\,(n-l-1)!}\,\frac{1}{(2l+1)!}}\,(2p)^{3/2}. \quad (10.8)$$

For the special cases of the 1 s-, 2 s- and 2 p-state, respectively, the radial wavefunctions take the simple form

$$v_{1s}(s) = (2\,|E|)^{-1/2}(2p)^{3/2}\,e^{-s/2}, \quad (10.9)$$

$$v_{2s}(s) = (2\,|E|)^{-1/2}(2p)^{3/2}\,(1-\tfrac{1}{2}\,s)\,e^{-s/2}, \quad (10.10)$$

$$v_{2p}(s) = (24\,|E|)^{-1/2}(2p)^{3/2}\,s\,e^{-s/2}. \quad (10.11)$$

In Fig. 22 the energy eigenvalue of the 1s-state and the 2s-state is plotted versus Z. Solutions for particle (solid lines) and antiparticle states (dashed lines) are indicated. $E(Z)$ displays the square root dependence according to (10.3). The radial density $\varrho\, r^2$ in units of fm^{-1} is shown in Fig. 23 for the 1s-state at the critical coupling strength $Z_{cr} = 274$.

11. The scalar square-well potential

In this chapter we discuss solutions of the Klein-Gordon equation for a scalar square-well potential

$$W(r) = -W_0\,\theta(R-r) \quad (11.1)$$

with the potential depth

$$W_0 = Z\,\alpha/R. \quad (11.2)$$

The calculations are identical to those presented in Chapt. 5 except for the obvious replacement

$$k_i^2 = E^2 - 1 + W_0. \quad (11.3)$$

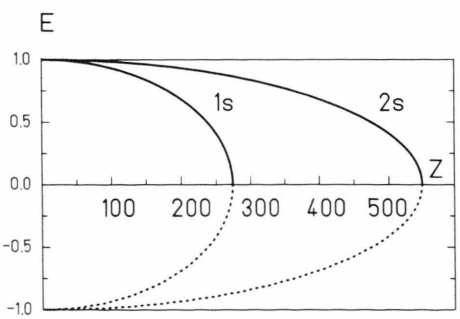

Fig. 22. The energy eigenvalue E of a Klein-Gordon particle in a scalar potential of the form $W(r) = -Z\,\alpha/r$. Solutions for particle (solid lines) and antiparticle states (dashed lines) are presented. E is displayed for the 1s- as well as for the 2s-state. The critical values for pair creation are $Z_{cr}(1s) = 274$ and $Z_{cr}(2s) = 548$.

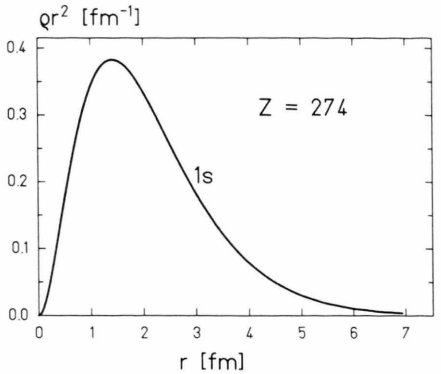

Fig. 23. The radial density $\varrho\, r^2$ in fm^{-1} versus r in fm of a pion in a scalar potential of the form $W(r) = -Z\,\alpha/r$. $\varrho\, r^2$ is shown for the 1s-state at the critical value $Z = 274$.

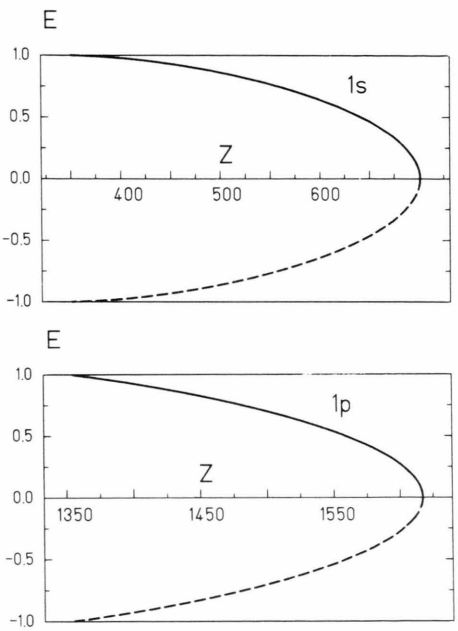

Fig. 24. The energy eigenvalue E of a Klein-Gordon particle in a scalar square-well potential with the range $R = 1$. The energies of the particle and antiparticle state are symmetric with respect to the border line $E = 0$. a) E for the 1 s-state. $Z_{cr} \simeq 701$. b) E for the 1 p-state. $Z_{cr} \simeq 1616$.

In the outer domain ($r > R$) Eq. $k_a = p$ still holds. In consequence we may take over all formulas of Chapt. 5) besides the normalization constant (5.12), in which the potential depth should be changed to $V_0 = 0$. The energy eigenvalues E of Klein-Gordon particles, which occupy the lowest angular momentum states ($l = 0,1$) in a scalar square-well potential, follow from the roots of (5.9) and (5.11), respectively. E is plotted in Fig. 24 for the 1s-state as well

as for the 1p-state. The energy eigenvalues for particle and antiparticle states are symmetric with respect to the border line $E = 0$. We obtained $Z_{cr}(1s) \simeq 701$ and $Z_{cr}(1p) \simeq 1616$.

12. Summary

We solved the Klein-Gordon equation for various types of short- and long-range potentials. Energy eigenvalues and normalized radial density distributions of spin-0 particles in spherical symmetric potentials are presented. Emphasis was laid on the determination of critical potential depths, i.e. the threshold for spontaneous pair creation. The appearence of antiparticle bound states in a restricted class of short-range potentials became plausible by illustrating the charge density components of the considered meson. The binding of an antiparticle obviously is caused by its particle constituents in the relativistic charge density whereas the antiparticle integral predominantly is located outside the potential range. This Schiff, Snyder, Weinberg effect does not occur in singular potentials. Furthermore, according to our numerical studies this surprising phenomenon was obtained only for s-states ($l = 0$). For a discussion based on more analytical grounds we refer to [30] and references therein.

Acknowledgement

One of the authors (G. S.) acknowledges the support of the Deutsche Forschungsgemeinschaft (Heisenberg Programm).

[1] W. Pieper and W. Greiner, Z. Physik **218,** 327 (1969).
[2] J. Reinhardt and W. Greiner, Rep. Prog. Phys. **40,** 219 (1977).
[3] Quantum Electrodynamics of Strong Fields, Ed.: W. Greiner, Plenum, New York 1983.
[4] L. I. Schiff, H. Snyder, and J. Weinberg, Phys. Rev. **57,** 315 (1940).
[5] J. Rafelski, L. P. Fulcher, and A. Klein, Phys. Rep. **38C,** 227 (1978).
[6] A. Klein and J. Rafelski, Z. Physik **A 284,** 71 (1978).
[7] A. Klein and J. Rafelski, Phys. Rev. **D11,** 300 (1975). For comments on this paper see [8–9].
[8] M. Bawin and J. P. Lavine, Phys. Rev. **D12,** 1192 (1975).
[9] A. Klein and J. Rafelski, Phys. Rev. **D12,** 1194 (1975).
[10] G. Calucci and G. C. Ghirardi, Nuovo Cim. **10A,** 121 (1972), **13A,** 1119 (1973).
[11] M. Bawin and J. P. Lavine, Nuovo Cim. **23A,** 311 (1974).
[12] S. A. Fulling, Varieties of Instability of a boson field in an external potential and black hole Klein paradoxes, unpublished report 1975.
[13] S. A. Fulling, Phys. Rev. **D14,** 1939 (1976).
[14] V. S. Popov, Sov. Jour. Nucl. Phys. **12,** 235 (1971).
[15] V. S. Popov, Sov. Phys. JETP **32,** 526 (1971).
[16] Y. B. Zeldovich and V. S. Popov, Sov. Phys. Uspekhi **14,** 673 (1972).
[17] A. B. Migdal, Sov. Phys. JETP **34,** 1189 (1972).
[18] M. Znojil, J. Phys. **A14,** 383 (1981).
[19] P. T. Ong, thesis, Institut für Theoretische Physik der Universität Frankfurt, 1976.
[20] W. Greiner, Relativistische Quantenmechanik-Wellengleichungen, Verlag H. Deutsch, Frankfurt 1981.
[21] A. S. Dawydow, Quantenmechanik, VEB Deutscher Verlag der Wissenschaften, Berlin 1967.
[22] L. I. Schiff, Quantum Mechanics, McGraw-Hill, 3rd edition, New York 1968.
[23] S. Flügge, Lehrbuch der Theoretischen Physik, Band IV, Quantentheorie I, Springer-Verlag, Berlin 1964.
[24] S. S. Schweber, An Introduction to Relativistic Quantum Field Theory, Harper & Row, New York 1961.
[25] L. D. Landau and E. M. Lifschitz, Quantenmechanik B. III, Akademie Verlag, Berlin 1974.
[26] M. Abramowitz and I. A. Stegun, Handbook of Mathematical Functions, Dover Publications, New York 1965.
[27] L. F. Shampine and M. K. Gordon, Computer Solution of Ordinary Differential Equations: The Initial Value Problem, Freeman, San Francisco 1975.
[28] Y. N. Kim, Mesic Atoms and Nuclear Structure, North-Holland, Amsterdam 1971.
[29] G. Soff, W. Greiner, W. Betz, and B. Müller, Phys. Rev. **A20,** 169 (1979).
[30] V. S. Popov, V. L. Eletskii, and V. D. Mur, Sov. Phys. JETP **44,** 451 (1976).